

A Review of Dynamic Models and Measurements in Golf

John McPhee

Received: date / Accepted: date

Abstract A narrative review of dynamic models of golf phenomena is presented, as well as current technologies for measuring the motions of a golfer, club, and ball. Kinematic and dynamic models of the golf swing are reviewed, including models with prescribed motions or torques as inputs, and predictive dynamic models that maximize an objective (e.g. driving distance) to determine optimal inputs or equipment designs. Impulse-momentum and continuous contact dynamic models for clubhead-ball and ball-ground impacts are described. The key observations from 172 cited references are extracted and presented, along with suggestions for future research.

Keywords Golf · Dynamic models · Measurement · Simulation · Review

1 Introduction

From 1980 to 2018, driving distances by professional golfers increased by 40 yards (36 m) [1]. As in other sports, this achievement was partially due to increased size and fitness of the athletes; the longest-driving professional golfers have become taller and heavier [2]. However, improvements in golf equipment design have resulted in even greater performance gains. As evidence, consider that many senior professional golfers in 2017 were driving the ball 10-28 yards (9-26 m) farther than they did when they were at their physical peak at age 30 [1,3], and that the top five senior professional drivers in 2020-21 hit the ball an average of 17 yards (16 m) farther than they did on the PGA Tour in 1995 [1]. Furthermore, jumps in driving distances have coincided with equipment

Funding of this work by the Canada Research Chairs program is gratefully acknowledged.

J. McPhee
Systems Design Engineering
University of Waterloo, Canada
E-mail: mcphee@uwaterloo.ca

innovations such as oversized metal clubheads and solid core golf balls [2, 4]. Design improvements to irons, wedges, and putters may also have contributed to performance gains, e.g. the mean number of putts per green in regulation on the PGA Tour dropped from 1.816 to 1.768 from 1986-2021; over 18 holes, this is a gain of almost one full stroke per round¹.

Engineers have developed new measurement technologies that provide quantitative feedback to golfers and coaches, who use this data to improve swing biomechanics and club fitting. High-quality measurements have also been used by researchers to develop dynamic models of the swing, impact, and subsequent ball flight; these models have been used to explore and develop new equipment designs, contributing to the improvements we have seen in clubs and balls [4]. Over the past 40 years, these equipment innovations have led to more United States Patents in golf than in all other sports combined [5, 6].

In this paper, a narrative review of research publications on dynamic models in golf is provided, the first such review paper since 2008 [4, 7–10]. The goal of this paper is to provide an overview of the state-of-the-art in golf dynamic models to researchers in the field, along with directions to specific works published in their areas of specialization. The paper begins with a study of technologies used to measure the dynamics of the golfer and their equipment, along with examples of their usage in the literature. Then, the structure of the paper follows the sequence of actions in a golf shot: dynamic models of the swing (Section 3) followed by impact (Section 4). Aerodynamic models of the golf ball are outside the scope of the paper. Unless stated otherwise, the golfer is assumed to be right-handed.

2 Measurement Systems

“Measure what is measurable, and make measurable what is not so.”

Galileo Galilei

Experimental measurements of golf phenomena are essential to understanding the underlying dynamics; these measurements provide value to golfers, coaches, and researchers alike. Furthermore, high-quality measurements are required to develop a dynamic model, to identify the parameters of the model, and to evaluate if the model results match physical reality. In this section, a review is given of the technologies used to measure the kinematics and dynamics of a golfer, golf club, and ball. Papers that demonstrate the use of these measurement technologies in golf are provided.

2.1 Golfer Measurements

Countless articles, reports, and books have been published on the kinematics of the golf swing, often based on subjective opinions of what constitutes an

¹ A green is reached in regulation if the number of shots required is 2 less than the par for the hole, e.g. 3 or fewer shots are needed to land on the green of a par-5 hole.

effective technique. In contrast, fewer studies have used motion capture equipment, kinematic equations, and software to determine the three-dimensional position and orientation (3D pose) of the golfer's body parts during the golf swing. This kinematic data is often complemented by force plate measurements of ground reaction forces (GRFs) between the feet and ground [11,12]. Using the pose and GRF data as input to a multibody skeletal model, one can calculate joint angles, speeds, and torques as functions of time (see Section 3.1), from which objective conclusions can be drawn [13]. Hume and Keogh [14] provided an overview of golf experiments that used motion capture, GRF, and other measured data to obtain meaningful insights into the golf swing.

The established method for tracking human movements is to use a multi-camera system that tracks physical markers (usually small spheres, see Fig. 1) attached to bony landmarks on different body parts [14,15]. The multi-camera images are then processed to obtain 3D positions of markers at any time; with multiple markers on a body segment, its 3D pose can be calculated for each video frame. Numerical differentiation of pose data provides translational and angular velocities. The 3D location of joint centers in a skeletal model can then be estimated, knowing the relative positions of body-fixed markers, after which joint angles and speeds can be determined from rigid body kinematics.

Many researchers have used marker-based camera systems to study golf swings. Chu et al [16] combined motion capture with GRF data to show that lateral weight-shifting and the X-factor (the relative axial rotation between the pelvis and upper torso) can influence ball launch speed, as can the rapid uncocking ("release") of the wrist just prior to impact (consistent with previous dynamic models [17]). Choi et al [18] used motion capture data to show that professional golfers have smoother swings than amateurs, where smoothness is characterized by kinematic jerk (the derivative of acceleration). Motion capture has also been used to determine the contributions of the pelvis and trunk to the putting stroke [19]. These experimental studies show the importance of including pelvis, shoulder, and wrist rotations in golf swing models.

Marker-based motion capture systems typically use infrared cameras that are calibrated for a lab setting. They are not very portable nor easy to deploy outdoors, markers may be occluded if too few cameras are used, and the markers may interfere with the natural swing of the golfer.

As an alternative to camera-based marker tracking, some authors have used electromagnetic tracking of sensors attached to body parts. Such systems do not require direct line of sight and need fewer sensors than camera-based systems for orientation calculations, but tend to have smaller capture volumes, larger sensors, and lower sampling frequencies, and are susceptible to field disturbances from metallic objects or electrical sources. Electromagnetic tracking was used by Neal et al [20] and Tinmark et al [21] to study the proximal-to-distal sequencing of joint kinematics in a golf swing; dynamic models have shown how clubhead speed is increased by this sequencing [22].

Inertial measurement units (IMUs) have recently seen growing adoption by golf researchers. These wearable sensors use accelerometers and rate gyroscopes to calculate the pose of body parts during a swing; advances in signal

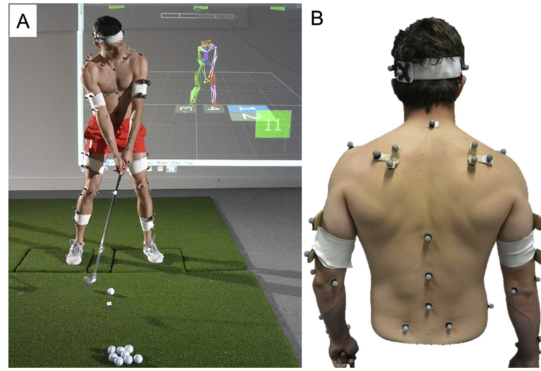


Fig. 1 A. Camera-based motion capture of golf swing with force plates under feet. B. Marker placements on back. Reproduced from [94]

processing over the past decade, including kinematic model-based Kalman filters, have reduced the drift error associated with IMUs [23]. Their position accuracy does not match that of marker-based systems, but IMUs can be deployed more easily in the field since they do not require external cameras nor transmitters. Similar to markers and electromagnetic sensors, wearable IMUs may affect the natural swing of the golfer. IMUs on the hand and upper arm have been used to distinguish amateur from professional golf swings [24] and to calculate the time-varying wrist angle [25], thereby providing real-time data to the player or coach on wrist release. However, Lückemann et al [26] cautioned that an IMU placed on the wrist did not give precise measurements of clubhead speed. Using data from IMUs on the head, left wrist, and pelvis, Kim and Park developed artificial intelligence (AI) algorithms to identify the timing of four key events in the golf swing [27].

Markerless motion capture from multi-camera RGB video recordings is an emerging technology for measuring the 3D kinematics of a golf swing. It can be seen as an advance on current algorithms that track a manually-identified point in a 2D video recording, which have been effective for sports video analysis [28]. Using multi-camera video recordings of a golf swing and AI algorithms, the current state-of-the-art being convolutional neural networks (CNNs), the 3D locations of joint centers (including occluded joints) are estimated at each video frame [29]. With a suitable skeletal model of known dimensions, the 3D pose of the golfer is calculated automatically. The need for calibrated multiple cameras limits the portability of these systems, but they can be used indoors and outdoors with natural lighting and, with no attached markers, the golfer is able to swing freely.

At the time of writing, several research groups are developing AI algorithms to track the 3D movements of golfers, using only one camera. Park et al [30] and Lv et al [31] used depth cameras to locate 3D human joint centers with a mean error of 2.9 and 1.7 cm, respectively. However, these infrared cameras are too slow to detect the moment of impact [32] and cannot be used outdoors.

In contrast, RGB video (e.g. from a smartphone) offers maximum ease of deployment both indoors and outdoors. McNally et al [33] developed a database of golf videos (GolfDB) and a CNN algorithm that identifies the timing of eight key events in the golf swing from single-camera RGB video images. Ko and Pan [34] used a CNN to calculate rotation angles for the pelvis, upper thorax, shoulder, and head from single-camera RGB images; the angles were estimated to within 4-5 degrees of measurements obtained from an IMU-based motion capture suit. State-of-the-art “lightweight” CNNs for human pose estimation can now be deployed on the processors in modern smartphones [35], but they are less accurate than the motion capture methods described above; given the pace of research in pose estimation [36], substantial accuracy gains are expected soon.

Strain gauges and pressure sensors can be used to measure the contact forces and moments exerted by the golfer on the grip. Koike et al [37] reported good agreement between these measurements and values calculated using inverse dynamic models (Section 3.1). Budney [38] found that the left fingers apply a relatively large force during the entire swing to counteract centrifugal club forces, while the right fingers apply impulsive loads during the downswing to accelerate the club. Using thin film force and pressure sensors, Komi et al [39] observed that individual golfers have a unique and repeatable grip force “signature”. Rather than these external sensors applied to the hand or club, one can imagine future force sensors being integrated into the construction of golf grips that have the same look and feel as traditional grips [40].

Several physiological variables can be measured during the golf swing. Electromyography (EMG) sensors can measure the activity of muscles that create the forces needed to swing a club [41, 42]; Verikas et al [43] used surface EMG measurements of the arm and shoulder muscles to predict clubhead speed. With recent advances in wearable sensors and AI algorithms, there are many opportunities to correlate golfing performance with signals from sensors that measure heart rate [44], brain activity [45], galvanic skin response, and other physiological signals. In future, these measurements might be synchronized on a smartphone with camera and GPS data that can be mined by AI algorithms to provide immediate feedback to the golfer.

2.2 Club and Ball Measurements

There are many static measurements of a golf ball and club that are needed for kinematic and dynamic models, including club length and loft angle, shaft flexibility, clubhead geometry and mass properties, and ball diameter and mass. Equipment to measure these parameters can be purchased or custom-built. To determine compliance with the Rules of Golf (specifically The Equipment Rules [46]), the R&A Rules Limited and the United States Golf Association (USGA) make static and dynamic measurements of golf clubs and balls, including clubface flexibility and coefficient of restitution, and ball carry distance for standardized launch conditions. The focus of this section is the measurement

of dynamic phenomena for the club and ball that supports the development and validation of dynamic models.

The same marker-based systems for human motion capture can also be used to measure the motion of a golf club (Fig. 2), provided the camera frame rate is high enough [47]. Researchers have used multiple high-speed cameras to track markers on the clubhead and ball [48–52], from which the clubhead velocity and orientation before and after impact can be calculated, along with the location of impact on the clubface. Marker-based measurements allowed researchers to investigate the effects of face orientation and impact location on the subsequent ball motion, and supported the development of dynamic impact models (Section 5).

Marker-based experiments were used by Haeufle et al [53] to show that mean clubhead speed did not decrease when heavier clubs were swung, in contrast to predictions by a simple model [54]. Using a similar setup, Worobets and Stefanyshyn found that the mean clubhead speed was unchanged for 40 golfers swinging shafts with five different stiffnesses [55]. However, subject-specific differences were found in 27 of the golfers, who had higher clubhead speeds with a more flexible shaft. This finding supports the idea that performance can be improved with a shaft tailored for the individual golfer [56], an idea promoted in subsequent model-based studies [57].

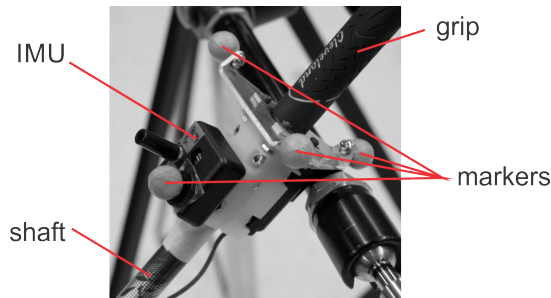


Fig. 2 IMU and optical markers attached to shaft below the grip. Reproduced from [23]

Multi-camera motion capture has also been used to track markers placed on golf putters, which only require three non-collinear markers on the club if shaft deflections are negligible; more markers can provide greater tracking accuracy [58]. Using three markers to measure putting motions that were then input to the 3D Newton-Euler equations, Shimizu et al calculated the corresponding grip forces and moments [59]. They observed that transverse forces and moments can cause rotation about the shaft axis, and that the golfer must apply a corrective moment about this axis to square the clubface at impact.

Researchers have tracked markers on both the driver clubhead and grip [60, 61]; from movement of the head relative to the grip, the time-varying bending deflections in the plane of motion (“lead/lag”) and perpendicular to this plane (“toe up/down”) were calculated. The results confirmed the expected forward

bend of the shaft (lead) at impact, which increases the effective loft at impact (the “dynamic loft”), plus a significant toe-down deflection (or “droop”) — results that are consistent with dynamic models of the flexible shaft [62,63].

Strain gauges mounted on the shaft can also be used to measure time-varying bending deflections and torsion during a golf swing [64,65]. These measurements support the development of flexible shaft models and have been validated against deflections calculated using a multi-camera marker-based system [60]. From strain gauges applied to both flat panels and golf shafts, Betzler et al showed that static material tests are sufficient to characterize the stiffness properties of shaft models used in dynamic swing simulations [66]. They also found that an individual golfer has a repeatable time-varying pattern of deflection, which is different from that of other golfers, again pointing to the existence of a unique swing signature [67].

IMUs have also been used to track the movement of golf clubs (Fig. 2). King et al developed a lightweight (25 g) wireless IMU fitted inside the grip of a putter [68]. Using kinematic transformations of IMU data, they computed the time-varying 3D pose of the clubhead to within 3 mm and 0.5 degrees, as well as the clubhead velocity and ball impact location. Other researchers have mounted IMUs on putters [69,70], but without validating their measurements. Jiao et al developed a CNN that uses data from strain gauges and an IMU to classify a full swing into one of nine types (e.g. slice, hook, pull) with a classification accuracy of 95% [71]. Recently, Lombardo et al placed a 20-gram IMU near the clubhead of an unspecified club; results were obtained for clubhead orientation during a swing, but results were not validated and the accelerometers saturated [72]. Future advances in hardware and software are needed before IMUs can accurately track the rapidly-changing 3D pose of a golf clubhead, especially drivers.

One can also measure the movement of a golf club or ball or both using portable devices that can be deployed indoors or outdoors. One such system uses three ultrasound receivers to track three transmitters on a golf putter, from which the 3D pose of the putter head was obtained with an accuracy of 0.1 mm and 0.1 degrees [73]. Ultrasound is susceptible to loud noises or strong winds, and has a limited capture volume that makes it appropriate for putting but not a full swing. An ultrasound system has been used to show that face angle has more influence on the direction of a putted ball than putter path or impact point [74], and to compare the performance of standard, long, and belly putters [75]. Another portable system uses four battery-powered non-coplanar LED lights, attached to a putter shaft, that are tracked by a camera-based system [76]. Similar to IMUs and ultrasound transmitters, the LED attachments add mass to the shaft (which may affect the stroke), and only the club motion is measured, not that of the ball.

In contrast, multi-camera systems deployed in a portable device can track visible features on a clubhead or ball or both using high-speed cameras and image processing algorithms to compute 3D poses and velocities. The measured ball launch conditions can be input to an aerodynamic model to compute ball trajectories [77], or to a ball-ground contact model (for putting, Section 4.3).

These stereoscopic “launch monitors” have become popular for use indoors as part of a golf simulator or for research [51,52], and for training outdoors. Radar-based technologies have also been deployed in launch monitors to track a substantial portion of the ball trajectory; clubhead conditions at impact are estimated using an impact model (Section 4). In newer launch monitors, radar and camera measurements have been fused to increase accuracy. Leach et al [78] compared radar-based and camera-based launch monitors, using high-speed camera measurements as the reference, and concluded that: (1) ball motions are measured with high accuracy but clubhead measurements may not be accurate enough for some research applications, and (2) either type of launch monitor provides sufficient accuracy to golfers, coaches, and club-fitters for the purpose of improving performance.

3 Multibody Dynamic Models of the Golf Swing

“All models are wrong, but some are useful.”

George Box

The human body has over 200 bones connected by 360 joints that are actuated by 650 muscles, all controlled by a complex and efficient nervous system. But for many people, this system meets its match when they try to swing a golf club such that it makes direct contact with the ball at high speed and with correct orientation. This is a challenging task due to the complexity of the golf swing, which requires highly-synchronized timing of multiple human joints [13]. Furthermore, the golf swing is sensitive to club design parameters such as shaft flexibility [60] and mass [79]. It is critical that the biomechanical characteristics of the golfer are addressed during the equipment design and selection process [80]; combined models of the golfer and club support the design of new equipment that improves athletic performance.

Many researchers have created biomechanical models of the golf swing, the last review of which was provided in 2008 by Betzler et al [9]. An updated narrative review is provided here, in which golf swing models are placed in one of three categories: (1) models for which the inputs are measured motions (kinematics), (2) models in which the inputs are manually-prescribed torques, and (3) predictive simulation models in which optimal control methods are used to obtain the dynamic inputs that maximize some objective function (e.g. driving distance). The third category is particularly interesting since these models represent virtual golfers that respond to golf club design changes (e.g. mass, shaft length) similar to a real golfer, as long as the model represents the biomechanics and club dynamics with sufficient accuracy. If that is the case, these predictive models can provide cheaper, faster, and more objective evaluations of new club designs than those obtained from human testing.

3.1 Models Driven by Measured Motions

Using motion measurements described in Section 2, one can create kinematic or inverse dynamic models that provide valuable metrics to the golfer or coach. Motion capture data can be combined with a link segment kinematic model to estimate joint angles and speeds, which provide insights into the proximal-to-distal “kinematic sequencing” of a golf swing [81]. Using estimates of the inertia properties of different body segments, an inverse dynamic analysis [82] can convert kinematic and GRF measurements into the driving torques at the different joints involved in the swing.

In 1967, Williams [83] used “multi-flash photography” of Bobby Jones’s golf swing to create a double-pendulum model, in which the upper pendulum represents the left arm (for a right-handed golfer) rotating about a fixed shoulder joint, and the lower pendulum is a rigid golf club rotating about the wrist joint (Fig. 3). From the dynamic equations, Williams was able to calculate the forces applied to the grip and the work done by the golfer, and investigate the role of the wrist joint in generating clubhead speed. He proposed that clubhead speed could be maximized by locking the wrist at the start of the downswing, and then letting the wrist freely unhinge (zero wrist torque) from the time of wrist release to ball impact. Cochran and Stobbs [84] also proposed a planar double-pendulum model of the golf swing, and used high-speed photography to show how the model was a good fit to the kinematics of elite golfers.

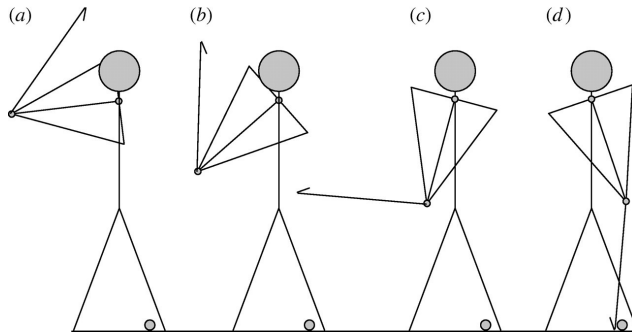


Fig. 3 Double-pendulum model of golf swing from top of backswing (a) to impact (d). Reproduced from [110]

In the 1980s, Vaughan [85] and Neal and Wilson [86] recognized that golf swings were not planar and created 3D inverse dynamic models. Vaughan used the measured club motion to calculate the force and torque applied by the hands, while Neal and Wilson used the arm and club motions to compute the shoulder and wrist torques during the swing; unlike Williams’s free-wheeling wrist joint model, they reported large positive values of wrist torque for elite golfers during the short interval (~ 40 ms) just before impact.

In the 1990s, researchers used measured grip kinematics as inputs to dynamic simulations of clubs with flexible shafts. Nesbit et al used this approach to investigate the effects of different iron clubheads on the deflections of the shaft, modelled as 15 rigid segments connected by 3D massless beams with stiffness and damping [87]. Sandhu et al used Rayleigh beam theory to develop a computationally-efficient analytical model of a shaft with variable geometry and stiffness along its length [88], the goal being to match the stiffness profile of the shaft to the swing of a given golfer. Furukawa et al used experimental measurements of a driver swing to determine the generalized forces and torques that should be applied to a finite element (FE) model of the shaft, to study the effect of grip acceleration on shaft deflections [89]. Tanaka and Sekizawa used an FE model of the carbon fiber structure of a driver shaft, with measured grip kinematics as prescribed inputs; the authors used this model to demonstrate the effects of torsional stiffness and impact timing on the clubhead orientation at impact [90].

Nesbit [91] created a 3D biomechanical model of the human golfer, using commercial multibody dynamics software (MSC.Adams), plus a flexible shaft modelled as 15 rigid segments connected by springs. Unlike most previous models with only a few driven joints (“degrees of freedom”, or DOF), Nesbit’s biomechanical model included 15 segments connected by 15 joints. The model was driven by experimental kinematics, and the computed outputs included the clubhead motion, shaft deflections, and joint torques and powers. Validation of the model was provided by good visual agreement between measured and computed ground reaction forces. Demircan et al [92] also created a biomechanical golfer model, using open-source modelling software (OpenSim); the torque-generating capacities of 100 muscle forces were used to compute maximum joint torques, which were then related to the acceleration of the clubhead (assuming a rigid golf shaft). The need for 3D models and analyses was firmly established by Smith et al [93], who showed that 2D analyses could result in large errors in kinematic variables like the X-factor.

Recent improvements to kinematically-driven golfer models include the work of Bourgain et al [94], who replaced a spherical joint model of a shoulder joint with a physiological model including scapula and clavicle, thereby increasing the fidelity of their OpenSim model. Choi and Park [95] tackled the inverse dynamic indeterminacy due to the closed kinematic chain formed by two arms gripping a club. In contrast to most works that only model the leading (left) arm, Choi and Park included both arms in their model and used measurements of grip force and torques to resolve the indeterminacy and solve for joint torques in both arms. Takagi et al [96] accomplished a similar feat for the lower body, using inverse dynamics and GRF measurements to solve for the torques in the leading and trailing ankle, knee, and hip joints.

Future research might use optimization methods instead of force measurements to resolve the redundancy in joint torques for closed kinematic chains in the golfer model, similar to what is currently done to solve the muscle redundancy problem, i.e. solving for the multiple muscle forces that contribute to the resultant torque at a joint [97]. By including detailed Hill-type models

[82] of muscles in future golfer models, instead of net joint torques, the contributions of individual muscles may be identified and used to improve golfer performance and reduce the risk of injury.

3.2 Forward Dynamic Models Driven by Prescribed Torques

The previous models offer useful insights into the kinematics and kinetics of a golfer, but they require motion measurements (as inputs) that may be expensive and difficult to obtain outside a research laboratory. To reduce the dependency on experimental movement data, some researchers have created forward dynamic models of the golf swing that are driven by manually-prescribed torques. The challenge here is to find and prescribe joint torques that create simulated movements that are representative of real golf swings.

Milne and Davis achieved this using strain gauge measurements on the golf shaft to determine appropriate values for shoulder and wrist torques in a double pendulum model of a driver swing [64]. Both torques were found to be ramp functions of time. The lower pendulum (the club) was modelled using analytical beam theory, and the simulation results were consistent with experiments that showed that (1) the shaft bends forward at impact, thereby increasing the dynamic loft for longer drives [60], and (2) the shaft flexibility has little effect on clubhead speed [55].

Jorgensen [98] applied shoulder and wrist joint torques to the rigid double-pendulum model of Williams, and provided a constant horizontal acceleration of the shoulder joint as an additional input to the two differential equations of motion. In his “standard swing” model of the downswing, the shoulder torque was constant and manually tuned to obtain simulation results that match high-speed photographs. Similar to Williams’s earlier model, the wrist provided a reaction torque that naturally decreased while maintaining a constant wrist cock angle; once this reaction torque went to zero, the wrist was released and the applied wrist torque was set to zero (free-wheeling). Jorgensen modelled the club flexibility using a rotational spring just below the grip; this simple model was sufficient to show forward bending of the shaft at impact. Pickering and Vickers [54] used a similar double-pendulum model with prescribed torques, but without shaft flexibility and with the teed ball not constrained to lie directly below the shoulder joint (as previous models assumed). They confirmed the observation that horizontal clubhead speed was maximized by teeing the ball ahead of the shoulder joint location, i.e. towards the left heel.

Chen et al [99] drew a similar conclusion about optimal ball position for maximum clubhead speed at impact, using a rigid double-pendulum model of the downswing in which constant values of the shoulder and wrist torque (after wrist release) were manually tuned. Consistent with the experiments of Neal and Wilson [86], they found that a positive wrist torque just before impact increased clubhead speed. Suzuki et al [100] also used a torque-driven double-pendulum model, but with a flexible golf shaft, and manually adjusted the timing parameters of piecewise linear torque functions at the shoulder and

wrist to maximize clubhead speed at impact. Suzuki et al [101] then included human torque limits in their shoulder and wrist torque functions, and modelled a 3D golf club with an Euler-Bernoulli beam model for the shaft (assuming constant properties along its length) and an offset point mass for the clubhead; the model was used to explore relationships between wrist torque timing, shaft bending, and clubhead speed.

More recently, Lee and Park [102] used a torque-driven double-pendulum model to estimate the rotation of the arm, given IMU measurements of the club rotation. The wrist torque was calculated from inverse dynamics of the club, while the shoulder torque was parameterized as a linear combination of arm angle and angular speed. The constant parameters were then tuned in a forward dynamic simulation until the club kinematics matched the IMU measurements. The result was an estimation of arm kinematics without directly measuring them, which showed the power of combining wearable sensors with dynamic models.

McGuan [103] used the MSC.Adams software to create a biomechanical model with many DOF and a continuous flexible shaft model. Joint torques were proportional to the difference between simulated and experimental joint angles. Thus, the control torques drove the motion to reproduce a recorded baseline movement, i.e. the simulation required kinematic measurements as input. By altering the control gains, the baseline swing could be modified by the simulation so as to maximize some objective (e.g. clubhead speed) for golf clubs with different mass or stiffness. Kenny et al [104] also used an MSC.Adams model, in which the prescribed joint torque inputs were obtained from an inverse dynamic analysis, i.e. measured kinematics were again required.

While kinematic-driven models remain popular for kinematic and inverse dynamic analysis, manually-tuned torque-driven models have become less popular as researchers have switched their attention to predictive dynamic models that do not require manual tuning or experimental data to perform “what-if” simulations of new swings or golf clubs.

3.3 Predictive Dynamic Simulation Models

Rather than manual tuning of joint torques, optimal control theory can be used to find the time-varying input torques/forces that maximize some objective function like clubhead speed or driving distance. The resulting simulation models are arguably more useful than kinematically-driven models, since they can be used to predict the effects of new golf club designs *in silico*; essentially, the virtual golfer will adjust their swing to optimize their performance for different golf club designs. In this way, the golfer’s swing can be optimized for a given club, or new golf clubs can be tested and optimized by a computer before prototyping and final evaluation by the golfer [105]. Of course, the determination of the optimal swing or club is limited by the fidelity of the dynamic model.

Rao [106] provided a detailed overview of the mathematical formulations and numerical methods used to solve optimal control problems (OCPs), which are classified as either indirect or direct methods. In an indirect method, the calculus of variations is used to convert the OCP into a boundary-value problem in which differential equations are solved while satisfying boundary conditions. In a direct method, the states or inputs or both are discretized in time, thereby converting the OCP into a nonlinear optimization method. There are commercial and open-source software packages available for solving an OCP using either an indirect (“optimize, then discretize”) or direct (“discretize, then optimize”) method. In a third approach, one might represent the time-varying input torques as parametric functions of time (e.g. polynomial with constant coefficients), which transforms the continuous OCP into a parameter optimization problem that is more easily solved.

The first predictive golf swing simulation was in 1975 by Lampsas [17], who used a 2D rigid double-pendulum model of the downswing and indirect optimal control methods to find the time-varying shoulder and wrist joint torques that maximized clubhead speed at impact. Lampsas obtained important insights into the golf swing, including the effects of club length and mass on the swing dynamics [77, 79], and the importance of a late wrist release for maximizing clubhead speed [101]. Campbell and Reid [107] also used indirect methods, but with torso rotation included in a 2D triple-pendulum (3-DOF) model of the swing, to solve for the torso, shoulder, and wrist torque inputs that maximized clubhead speed without exceeding joint torque limits. Similarly, Kaneko and Sato [108] combined indirect optimal control methods with a 3-DOF triple-pendulum model of the downswing to study the effects of club mass and inertia on the swing, and to find torso, shoulder, and wrist torques that minimized joint torques or powers. They found that the minimum-power torques were a good visual match to plots of experimental torques, but this may be because the experimental values were used as the initial guess for the OCP, which may have converged to a local optima near the initial guess.

In a parameter optimization approach, Ming et al [109] used Fourier series to represent the shoulder and wrist joint torques in a double-pendulum model with flexible shaft; the Fourier coefficients of the optimal joint torques were obtained by minimizing either mechanical work or the derivatives of joint torques. Consistent with Kaneko and Sato, they found that minimizing mechanical work provided a better match to human swings. Using 2D double- and triple-pendulum models of the downswing, with a rotational spring to represent shaft bending, Sharp [110] parameterized the input torques using linear and hyperbolic tangent functions of time. Parameter optimization provided the input torques that maximized clubhead speed. As with other approaches that only consider clubhead speed, and not clubhead conditions at impact (e.g. angle of attack, dynamic loft, face angle), the resulting ball launch conditions were likely not optimal. Examining the Supplementary Material from Sharp, it seems that the shaft was not bending forward at impact and the clubhead had a negative angle of attack, neither of which is conducive to maximizing the driving distance.

Springs and Neal [111] used a 2D rigid triple-pendulum model of the downswing, with torques applied to the torso, shoulder, and wrist joints. Notably, they were the first to use “muscle torque generators” (MTGs), parametric functions of time that captured the activation and force-speed behaviour of human muscles:

$$T(t) = T_{act} \frac{(\omega_{max} - \omega)}{(\omega_{max} + \Gamma\omega)} \quad (1)$$

in which the active muscle torque was given by:

$$T_{act}(t) = T_{max} \left(1 - e^{-t/\tau}\right) \quad (2)$$

where $T(t)$ was the time-varying joint torque at time t following muscle activation, T_{max} was the maximum isometric torque achievable by the human, τ was the muscle activation time constant, ω and ω_{max} were the joint angular speed and its maximum possible value, respectively, and Γ was a constant shape factor for the torque-speed equation (1). This relationship for concentric muscle contractions captured the phenomenon that muscle forces decrease with increasing speed of contraction, which affected the maximum torque achievable at different points along the golf swing. Springs and Neal used parameter optimization to find the muscle firing pattern that maximized clubhead speed, and showed that unrealistic results are obtained when the properties of muscles are ignored in the torque functions.

In a followup paper, MacKenzie and Springs [22] extended the 2D model to a 4-DOF model that included forearm pronation/supination and allowed the torso and shoulder to rotate about non-parallel axes, resulting in a 3D golf swing. The active torque equation (2) was augmented with a second term that allowed deactivation of a muscle during the downswing. The flexible shaft was modelled as four rigid bodies connected by rotational spring-dampers, and parameter optimization was again used to find the muscle timings that maximized horizontal clubhead speed, but with the additional constraint that the clubhead should be aligned with the target at impact. The model results were in good agreement with experimental swings by an elite golfer, with root mean squared errors of 0.66, 1.25, and 1.53 degrees for the arm, torso, and club angles. The authors used their 3D model to (1) confirm the proximal to distal sequencing of joint torques (i.e. torso-shoulder-forearm-wrist) for maximum clubhead speed [111], and (2) show that shaft flexibility affects clubhead orientation at impact, but not clubhead speed [55,62]. The model was also used to demonstrate the effect of clubhead centre of mass location and radial grip force on shaft deflection [112]

Balzerson et al [113] further extended this model by including the passive stiffness and damping properties of human joints [114], replacing the discrete shaft model with the continuous flexible beam model of Sandhu et al [88], and including models of aerodynamic drag on the clubhead, clubhead-ball impact, and subsequent ball trajectories. In this way, they optimized the muscle timing (and teed ball position) that maximized ball carry distance, not just clubhead speed, i.e. the full set of clubhead kinematics at impact were

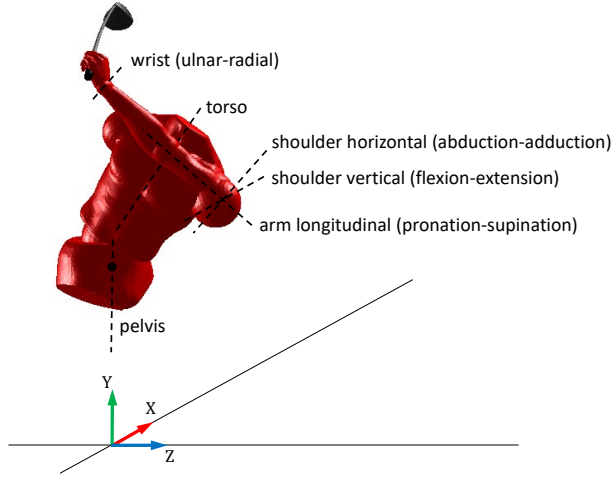


Fig. 4 Dynamic 3D model of 6-DOF golfer, flexible shaft, and rigid clubhead. Reproduced from [116]

optimized. Brown and McPhee [115] used the Balzerson model in the first application of direct collocation optimal control to the golf swing, again with the goal of maximizing carry distance. Instead of restricting an MTG to a single activation/deactivation during the downswing, the optimal time-varying muscle activation torque $T_{act}(t)$ was computed directly.

McNally and McPhee [116] extended the model of Balzerson et al to six DOF, including two rotations at the shoulder (adduction-abduction and flexion-extension), and a separate rotation at the pelvis (Fig. 4), thereby allowing the X-factor to be represented. Unlike previous models, the backswing was also included in the dynamic simulation, which captured the energy stored in shaft bending and muscles/joints at the top of the backswing. This required the extension of equation (1) to include eccentric muscle contractions for negative joint speeds during the backswing. Again, parameter optimization provided optimal muscle timings and teed ball position, with the results in close agreement to the swings obtained from experiments with 10 elite golfers. This predictive simulation model, along with an experimentally-validated golf shaft model [63], was used to investigate the effect of shaft balance point on clubhead speed [57]. Ferguson et al [117] used a similar model to predict the reduction in carry distance caused by a reduced driver length (from 48 to 46 inches, in line with the recent Model Local Rule by the R&A and USGA). These examples are illustrative of the many what-if investigations that are made possible by a validated predictive simulation model.

Existing predictive dynamic simulations of the golf swing neglect the movement of the lower legs, so future models should include additional DOF to capture the important contributions of lower limb muscles [96]. If joint reactions are required (e.g. to study injury mechanisms), then the joint torques or MTGs

should be replaced with muscle models, including activation and contraction dynamics and musculoskeletal geometry [82]. The trailing arm should also be included in predictive simulation models, with optimization used to resolve the redundancy in driving torques or forces. If the cost function includes ball launch conditions (or driving distance), then efficient models of clubhead-ball impacts will be required (Section 4). The objective function might include more than driving distance; “smooth” swings might be obtained by including kinematic jerk in the cost function [18]. Direct collocation methods for optimal control have become popular in dynamic simulations of human gait [118], and their use in predictive golf simulations should be explored further. Given that an optimal control method requires many dynamic simulations for convergence, a future challenge will be to capture important biomechanical and dynamic phenomena in models that are computationally efficient and of sufficient accuracy to draw meaningful conclusions from the simulation results.

4 Dynamic Models of Ball Impacts

A golf swing requires a second or two to deliver the clubhead to the ball, after which impact occurs and the timescale of the underlying dynamics decreases by three orders of magnitude. The clubhead-ball impact occurs in less than 1 ms, during which time the ball goes from rest to its launch conditions, which in turn determine the subsequent ball flight. Engineers have achieved major advances in golf equipment design over the past few decades to launch golf balls farther and straighter [119]. During the period of 1980-2018, when professional driving distances increased by 40 yards (30 m), metal driver clubfaces and solid-core golf balls were introduced to increase the efficiency of impact, along with lightweight graphite shafts to increase swing speed and oversized clubheads that reduce sidespin and ball speed loss on off-centre impacts.

These advances in equipment design were facilitated by dynamic models of clubhead-ball impact, which can be discrete models using the impulse-momentum principle and a coefficient of restitution, or continuous models in which normal contact and tangential friction forces are represented explicitly [120, 121]. These two approaches to clubhead-ball impact modelling are discussed in the next two subsections, followed by a review of dynamic models of a golf ball hitting the ground or rolling on a putting green.

4.1 Impulse-Momentum Models

By integrating Newton’s second law with respect to time, one obtains the impulse-momentum (IM) principle, which states that the change in momentum of a body is equal to the time integral of applied forces (the “impulse”). IM models are well-suited to impact problems in which the bodies have negligible displacements during an impact that is brief, which is the case for a clubhead striking a ball. However, they do not represent the ball or clubhead

deformations explicitly, and time-varying values of the normal contact and tangential friction forces are not available from IM models [122,123].

Winfield and Tan used an IM model to represent a ball struck by a driver with a 3D ellipsoidal clubface, which captured the effects of bulge and roll [124]. Taking the scalar components of the vectorial IM principles for translational and rotational motions, they obtained six equations for the ball and six for the clubhead. A 13th equation was obtained using the coefficient of restitution (COR) to relate the ball and clubhead speeds along the axis normal to the clubface; the Rules of Golf limit this COR to 0.83 with the intention of limiting driving distances [46]. Finally, two more equations were obtained by assuming that the ball is rolling on the clubface at the end of impact; this allowed the tangential speeds of the points in contact to be equated. With these 15 linear equations, the authors solved for 15 unknowns: the clubhead velocity (three components) and angular velocity (three components) after impact, the ball velocity and angular velocity, and the three components of the impulse vector.

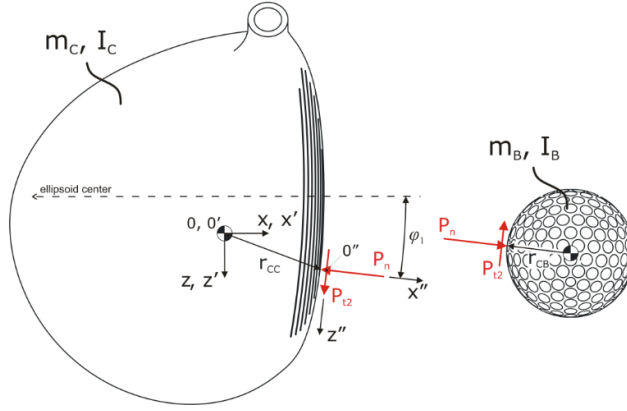


Fig. 5 Ellipsoidal clubface striking spherical ball, showing the normal and tangential components of linear impulse \mathbf{P} acting at the contact location. Vertical moment of inertia (MOI) of the clubhead is about a vertical Y axis through the centre of mass, while heel-toe MOI is about the horizontal Z axis. Reproduced from [127]

Using this model, Winfield and Tan determined the clubhead angle of attack (angle from ground plane to clubhead velocity vector, at impact) that maximized driving distance, for drivers with different loft angles. The authors assumed that impacts occurred at the “sweet spot”, the point on the clubface through which the normal axis intersects the clubhead centre of mass (CoM). With this assumption, and neglecting the shaft so that the clubhead was essentially a free-flying body, the ball was launched with zero sidespin and the resulting trajectory was 2D.

Also using the 2D version of Winfield and Tan’s IM model, and assuming a horizontal clubhead velocity (zero angle of attack), flat clubface, and sweet spot impacts, Penner obtained an analytical solution for the 2D ball launch conditions [125]. The COR was a function of impact speed and angle, and a constant angle (3.3°) was added to the clubhead loft to account for forward deflections of the shaft (the dynamic loft). Using models of the ball aerodynamics and its run on the ground after landing, the author found the clubhead loft that maximized total driving distance (carry + run) as a function of clubhead speed; the recommendation that higher lofts be used for slower swing speeds is now widely used by club fitters.

The full 3D IM model was used in several subsequent investigations [126–128]. Penner studied the effect of driver clubface bulge on impact and the resulting ball trajectories [126]. The clubface was assumed to be a cylinder, with constant bulge and zero roll. Assuming zero angle of attack and using 3D versions of the aerodynamic and run models from [125], the author determined the bulge required to return the ball to the centre of the fairway, for impacts that were located 2 cm from the sweet spot (towards the toe). Penner found that the optimal bulge radius increased for larger values of clubhead volume and mass, and for slower clubhead speeds. Petersen and McPhee investigated ball speed, backspin, and sidespin for impacts at different locations on the clubface; they confirmed that moving the CoM towards the heel or toe produces draw-biased or fade-biased drivers, respectively [127]. Dewhurst examined the effects of driver design parameters like hosel location, moment of inertia (MOI) about the vertical axis, and COR on ball trajectories for centre-face and off-centre impacts [128].

Lindsay combined IM principles with the assumption of ball rolling on a flat clubface to model the 2D impact (in a vertical plane) by a putter [129]. He used this model to study the reduction of initial backspin by appropriate selection of putter loft and inertial properties, the goal being to minimize the initial sliding distance that precedes pure rolling of the ball. Lindsay concluded that a putter should have a low MOI about the heel-toe axis, and a low CoM location that increased the vertical gear effect². Brouillette replaced Lindsay’s rolling assumption with a friction model, and investigated the effects of different face treatments on friction and ball spins [130]. From experiments, he observed that face treatments such as inserts and grooves changed the contact forces but, for a given putt length, they had no effect on the ball skidding distance. Lambeth et al used experiments and a 2D IM model (in the horizontal plane) to conclude that deviations from the desired ball launch direction for off-centre impacts are minimized by maximizing the vertical MOI and minimizing the distance from the putter face to the CoM (CoM “depth”) [131].

² The “gear effect” refers to the tendency of the clubhead and ball to rotate in opposite directions following impact. In Fig. 5, the horizontal gear effect implies that a clubhead rotating clockwise after impact will impart a counter-clockwise spin to the ball, and vice versa. For impacts above the sweet spot on the clubface, the vertical gear effect reduces the amount of backspin caused by the club loft.

Cross used the IM principle to study 2D impacts of a golf ball with a clubhead or fixed flat plate [132]. Instead of assuming pure rolling of the ball when it leaves the clubface, Cross introduced non-dimensional quantities to obtain a sufficient number of equations for solution. One such quantity (λ) was the friction impulse divided by the normal impulse:

$$\lambda = \frac{\int F dt}{\int N dt} \quad (3)$$

where $\lambda \leq \mu$, the dynamic coefficient of friction ($\lambda = \mu$ for pure sliding contact). Another non-dimensional quantity introduced by Cross was the “tangential coefficient of restitution”, e_t , which was analogous to the COR but in a tangential direction, i.e. it was the ratio of relative tangential speeds of the points of contact after and before impact [133]. Like COR for the normal direction, e_t represented energy loss due to tangential deformation of the ball; if $\text{COR} = e_t = 1$, energy was conserved during impact. Unlike COR, e_t could take either positive or negative values, and could capture the phenomenon of the friction force changing direction during impact. By setting $e_t = 0$, the special case of pure rolling of the ball was obtained. A drawback of using the non-dimensional λ or e_t was that they are not constant parameters, but functions of the relative orientations, speeds, spins, and properties of the ball and clubhead/plate. Cross provided experimental values of λ and e_t for different ball/surface pairs and impact conditions, and derived the analytical relationship between λ and e_t [132].

Dewhurst challenged the long-held assumption that the shaft can be neglected in clubhead-ball impacts, after noticing that ball speed was greater than that predicted by his IM model for impacts near the shaft [128]. For central impacts, he endorsed the recommendation by Cross and Nathan to add one quarter of the shaft mass to the clubhead [134]. For off-centre impacts, Dewhurst suggested that the problem “may be beyond reasonable modeling methods”. To tackle this problem, McNally et al developed a dynamic model of a driver that included both a flexible shaft and clubhead [135]. From simulations corroborated by experiments, they also concluded that the force and torque applied to the clubhead by the shaft can not be neglected; these reactions created a stiffening effect that helped maintain clubhead speed and orientation through impact. Danaei et al [136] adjusted the 3D IM model to account for the missing shaft, by increasing the clubhead mass by less than 5% of the shaft mass — much less than the 25% previously recommended [134]. They also accounted for ball deformations by moving the ball CoM by about 0.5 mm, which resulted in the generation of ball rifle spin about the normal axis. These modifications provided accurate ball speed predictions (mean error < 0.03 %) and reduced backspin and sidespin errors by 85%, but further improvements to the accuracy of IM models (especially for sidespin) to capture shaft effects and ball deformations would increase the utility of these computationally-efficient tools for designing new driver clubheads [137].

4.2 Continuous Contact Models

Unlike IM models, continuous contact models use explicit representations of the normal force and tangential friction force between clubface and ball. By solving the differential equations of motion for the time-varying contact forces and deformations during impact, additional insights can be gleaned into the effects of clubhead design parameters on ball launch conditions.

If the geometry and material properties of the clubhead and ball are known, FE models can be created to determine the normal force and clubhead and ball deformations during a central impact. By supplementing these FE models with appropriate models for friction, oblique impacts can be simulated [138]. Chou et al combined a 2D FE model with a Coulomb friction model to study the oblique impact of a 2-piece ball on a rigid plate [139]. In agreement with experimental results, the computed COR was found to decrease with increasing impact speed, and a rougher surface gave higher ball spins than smoother surfaces for high angles of impact, i.e. typical of those for wedge shots. Tavares et al used a 3D FE model (plus Coulomb friction) of a multilayer golf ball being struck by a rigid clubface; they showed that a soft outer cover over a hard inner layer can provide lower spins to maximize distance with low-lofted clubs, and higher spins with higher-lofted clubs used near the green [140]. Iwatsubo et al used 3D FE models of a driver and 2-piece ball, with Coulomb friction, to simulate the ball launch conditions for impacts at various locations on the clubface. They confirmed that a larger vertical MOI, or a smaller CoM depth, resulted in less sidespin from off-centre impacts [141].

The previous FE models all neglected the shaft during impact. To investigate the role of the shaft, Tanaka et al [142] constructed prototypes and FE models of a flexible shaft connected to simple cylindrical clubheads being impacted by a ball fired from an air cannon; a Coulomb friction model was again used. The authors obtained good agreement between FE and experimental results, which showed that the shaft had the effect of reducing the variation in ball rebound angle, speed, and spin rate for different off-centre impacts.

FE models of the clubhead have been used to optimize the variable thickness across the clubface [143–145], the goal being to minimize the loss in ball speed resulting from off-centre impacts. FE models of the clubhead have also been combined with boundary element methods to predict the sound made by a driver [146, 147]; this sound has a strong influence on the golfer's perception of the club performance [148], so manufacturers design the clubhead structure to give a desirable sound of impact.

It is clear that FE modelling is a powerful design tool for investigating the structure and material properties of clubheads and balls. However, FE impact simulations can be time-consuming, especially when many iterations are required in an optimization algorithm used for design or predictive simulations, and are difficult to integrate with a multibody dynamic model of the golfer and club. As a result, researchers have developed analytical models of the time-varying contact loads, in an effort to achieve both accuracy and computational efficiency. Some of these researchers used Hertz contact theory, in which the

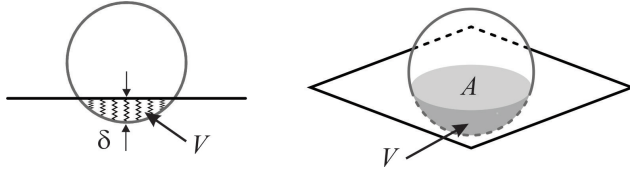


Fig. 6 Variables used in continuous contact models: δ is depth of penetration, A is contact area, V is volume of interpenetration (shaded). Reproduced from [150]

normal force is proportional to the indentation depth (deformation) raised to the $3/2$ power — essentially a nonlinear spring model. To capture the loss of energy during impact, Hunt and Crossley [149] added viscoelastic effects to this model of the normal force N :

$$N = k\delta^n + c\delta^n \frac{d\delta}{dt} \quad (4)$$

where k and c are the stiffness and damping constants, respectively, n is typically $3/2$, and δ is the indentation depth (see Fig. 6).

Dissatisfied with the accuracy of their IM model for balls impacting a rigid plate, Lieberman and Johnson developed 1D ball impact models comprised of two masses making up the ball, connected by nonlinear springs and a linear damper [151]. Their predictions of rebound velocity and normal force were in good agreement with experiments. They then combined this model with a 2-piece torsional model of the ball — consisting of a core and shell connected by a torsional spring and damper, and acted upon by Coulomb friction — to simulate oblique ball impacts. For lower angles of impact typical of lower-lofted clubs, they observed sliding of the ball followed by rolling, and a reversal of the friction force during impact [152]. Cochran also developed 1D models of near-normal golf ball impacts with a plate or flexible clubface, but used a Hunt-Crossley model for the force between the two masses comprising the ball; close agreement with experimental results was found for the normal force, rebound speed, and contact duration [153].

Arakawa et al showed that predictions of maximum normal force by Hertz theory were in good visual agreement with plots of experimental measurements [154]. To model oblique impacts, Arakawa expressed the friction force F as a function of the normal force N and the time-varying contact area A :

$$F = \mu N + \mu\eta \frac{dA}{dt} \quad (5)$$

where η was a constant that scaled the time derivative of A ; the second term allowed for a friction force reversal when $dA/dt < 0$ during rebound. For a single impact angle, calculations of time-varying spin from this model were in good visual agreement with plots of experimental spins at 28 m/s impact speed, but less so at 61 m/s [155]. More recently, Arakawa assumed the friction force to be proportional to A and the relative sliding velocity, and obtained a better agreement to experimental spins; the model was not predictive, since

measurements were needed to get the time-varying area A appearing in it [156].

Gonthier et al developed a volumetric model of normal impact force, which was obtained by integrating Hunt-Crossley contact forces over the contact area; the resulting force was proportional to the indentation volume V (see Fig. 6), not depth δ [157]. McNally et al [135] modelled oblique impacts between a clubhead and ball using this volumetric model and a regularized Coulomb friction model [158], which allowed smooth transitions between static (sticking) and dynamic (sliding) friction. The results were in good agreement with experimental drives by elite players, with mean errors of 0.17 km/h in ball speed, 0.93 deg in launch angle, and 150 rpm in backspin. Even with a flexible shaft included in the 3D dynamic model, the impact simulations were sufficiently fast to be used within predictive simulations of the golf swing.

Maw et al recognized that some parts of the contact patch may be sticking during impact of a ball on a flat surface, while others are sliding [159]. They assumed elastic ball properties (normal and tangential) and represented the contact area as concentric rings; $F = \mu N$ was used for rings that were sliding, and lateral displacements of ball and surface were equated for rings that were sticking. This introduced time-consuming iterative checks at each timestep of a simulation, but the model captured experimental phenomena such as the friction reversal for low-lofted clubs. The golf ruling bodies (USGA and R&A) used the Maw model in their study of spin generation by irons with different groove shapes, and obtained strong agreement between simulated and experimental values of normal and tangential forces [160]. Henrikson et al reduced initial clubhead speeds in the Maw model to compensate for the lack of energy dissipation in normal forces [161]. Their results were in good agreement with experiments (mean absolute error of 1 degree on rebound angle from an inclined plate), and showed the effects of clubhead-ball parameters (e.g. face angle and friction) on ball launch conditions. Future extensions to the Maw model might include different coefficients of friction for sticking and sliding, and a viscoelastic Hunt-Crossley model of the normal force.

Caldwell and McPhee compared four impact models to experimental data for drivers, and concluded that there is room for improvements in the accuracy of IM and continuous models, especially for ball sidespin predictions [137]. Future models may use trained neural networks to compute contact forces relatively quickly from the impact conditions [162]; accuracy will depend on the amount of data available for training. Apart from [132, 160, 161], there seems to be little work published on the modelling of ball impacts with irons or wedges, especially the prediction of sidespin and rifle spin, which represent additional opportunities for future research.

4.3 Ball-Ground Contact Models

After launched, the ball will eventually impact the ground, flagstick, or hole (ideally). Several dynamic models have been proposed for balls landing on the ground, rolling on a green, or interacting with the hole or flagstick.

In an early and comprehensive study of ball motions in sports, Daish developed an IM model of golf balls landing on a flat ground [122]. He used a constant COR of 0.5 to calculate vertical rebound speeds, and conditions of pure sliding or rolling (as appropriate) to determine horizontal ball motions. His model was able to predict the sharp halt of a ball hit into a green with high backspin by a wedge.

Penner used a similar IM model for ball bounces, but with the COR decreasing with impact speed, and assumed pure rolling conditions for a ball hit by a driver and landing on a flat fairway [126]; following a series of bounces of decreasing height, the distance rolled by the ball was determined using a rolling resistance model. The total ball run was the sum of the bouncing and rolling distances. In a followup paper, Penner accounted for the deformation of the ground during ball impact [163]. This “pitch mark” caused the impact surface to rotate by an angle θ_c that depended on impact speed and angle. By rotating the flat plane by θ_c , the previous IM model could be re-used, resulting in higher rebounds that better matched experimental observations. Penner found that the dominant factor that determined the total run of a drive was the ball angle of impact with the ground. Using experimental data, the USGA and R&A recently endorsed this conclusion and observed that the total run could be accurately modelled as a linear function of the angle of impact [164].

Haake [165] used high-speed photography to measure incoming and outgoing velocity and spin of golf balls launched downwards into different greens. Depending on its characteristics, each green was classified into one of two types: “rolling” greens for which the ball tended to rebound with topspin, and “slipping” greens in which the ball retained backspin after impact if the incoming backspin was high enough. Using this experimental data, Haake developed a continuous 2D viscoelastic model of the rigid ball impacting a two-layered turf, with the upper layer (grass and roots) represented by Kelvin-Voigt models in the vertical and horizontal directions, and the lower layer (soil) by dampers. The model was able to predict the first two bounces of the ball and the subsequent forward or backward roll. Roh and Lee used the IM model of Penner [163] to study balls landing on fairways or greens; they concluded that balls can bounce forward on firmer greens before running backwards, and the direction of bounce depends on backspin and green friction [166]. In future, it would be interesting to study the 3D motion of balls impacting greens with both backspin and sidespin.

About 40% of shots by players on the PGA tour are putts; given the importance of putting, several models have been developed for balls moving on greens. Daish presented a model of the initial sliding motion of a putted ball [122], while Penner provided a detailed analysis of the subsequent rolling motion [163]. Similar to a rolling tire, the normal force under a rolling ball acts

slightly ahead of the CoM, thereby creating a rolling resistance moment that slows the ball. Assuming a constant resistance, Penner modelled the trajectories of balls rolling on inclined greens, and solved for the initial ball launch conditions that resulted in a holed putt. He concluded that downhill putts are easier to hole than uphill putts, and that using the smallest possible launch speed on a sidehill putt gives the largest probability of holing the putt [163]. More complex expressions for rolling resistance were proposed by Hubbard and Alaways [167] and Roh and Lee [166], as functions of the ball speed and green Stimpmeter³ reading [168], respectively. Daemi et al modelled the impact with a zero-loft putter, the initial skid, and subsequent rolling motion on an inclined surface of a ball with offset CoM [169]. The authors found that small imbalances of the ball had little effect on launch conditions, but caused putts to be missed that would otherwise have been holed.

Holmes investigated the dynamic phenomena that occur when the ball interacts with the hole [170]. He solved the equations of motion for balls rolling on the rim, and developed IM models for balls striking the rim of the cup. Holmes used these models to predict the maximum capture speed for centre-face and off-centre putts, which were confirmed by experiments, and concluded that balls with higher MOI are harder to capture. Penner extended the Holmes model to account for inclined surfaces [163]. Kuchnicki included impact with the flagstick in the Holmes model, given the 2019 rule change that allowed the flagstick to remain in the hole during putting [171]. Consistent with the experimental study by Mase [172], Kuchnicki concluded that fewer putts were made with the flagstick left in the hole, except for central impacts by a putted ball whose speed was too great for holing without the flagstick.

5 Conclusions and the Future

“Prediction is very difficult, especially about the future.”

Nils Bohr

A narrative review of dynamic modelling research and measurements in golf has been provided. Current technologies to obtain kinematic and dynamic measurements of the golfer, shaft, clubhead, and ball have been described, along with research papers that demonstrate the use of these measurements. Dynamic models of the golf swing have been categorized as models driven by prescribed motions or torques, or fully predictive models that support “what-if” simulations of virtual golfers that respond to golf club design changes. Both impulse-momentum and continuous contact models of clubhead-ball and ball-ground impacts have been reviewed. Many of the predictions from these swing and impact models have been accepted by golfers and the golf industry, and models are now commonly used by manufacturers to design new clubs.

³ A Stimpmeter is a ramp that launches a ball with a repeatable speed on a green; the distance travelled (in feet) is the Stimpmeter reading of green speed.

From this review, some promising directions for future research have emerged. Combining multiple lightweight wearable devices with smartphones and machine intelligence could provide quick inexpensive feedback to players and coaches [27, 69, 71]. Sensors on the golfer or club might be replaced by markerless motion capture of golf swings indoors and outdoors, thereby freeing up the player to swing more naturally. These non-invasive camera-based measurements may be achieved through the deployment of AI algorithms onto smartphones with powerful processors, which may in turn support swing improvements and club fitting [56]. Subject-specific musculoskeletal models of the golf swing, including full muscle models, may be developed to match equipment characteristics to the individual player. Experimental validation of the integrated model of player and club will be essential, and advances in dynamic models of hand-grip interactions will be required. The ability of predictive simulations to test new golf clubs *in silico* may be enhanced by the use of direct collocation to solve the optimal control problem; objective functions that include criteria other than driving distance may generate smoother swings that resolve kinematic and muscle redundancies. Better models of impact with friction are needed to design the next generation of clubheads, especially irons and wedges. AI algorithms might be used to develop data-driven models of golf ball impacts and aerodynamics that simulate quickly, for deployment on launch monitors or golf simulators using virtual or augmented reality technologies.

Following the great success of his landmark treatise (Search for the Perfect Swing [84]) and four subsequent World Scientific Congresses of Golf, Cochran reviewed the current state of golf equipment technology in 2002 and made some predictions for the future — many of which are still relevant today [4]. In particular, improvements in golf equipment are limited by the Rules of Golf and the laws of physics; once these limits are reached, further increases in distance and accuracy can only come from the players themselves.

Acknowledgements The author is grateful to his graduate student co-authors (see References) for many years of enjoyable research collaborations and discussions. The author is indebted to the pioneers of golf research, including Tait, Williams, Daish, Lampsa, and Cochran, for their seminal contributions. The ongoing support of the Equipment Editors (Mike Stachura, Mike Johnson) at Golf Digest is gratefully acknowledged, as is the encouragement and patience displayed by the Editor-in-Chief (Tom Allen) during a pandemic.

Conflict of interest

The author declares that he has no conflict of interest.

References

1. PGA Tour Statistics. <https://www.pgatour.com/content/pgatour/stats/>. Accessed: 13 March 2022.

2. Bejan A et al (2013) The constructal evolution of sports with throwing motion: baseball, golf, hockey, and boxing. *Int J Design Nature Ecodynamics* 8:1-16. <https://doi.org/10.2495/DNE-V8-N1-1-16>
3. Myers A (2017) You won't believe how much farther PGA Tour Champions players are hitting the ball now than in their primes. <https://www.golfdigest.com/story/you-wont-believe-how-much-farther-pga-tour-champions-players-are-hitting-the-ball-now-than-in-their-primes>. Accessed: 13 March 2022.
4. Cochran A (2002) The impact of science and technology on golf equipment — a personal view. In: Ujihashi S, Haake S (eds) *The Engineering of Sport 4*, Blackwell Science, 3-15.
5. Schupak A (2018) Golf is the no.1 U.S. sport ... for patents. <https://www.ngf.org/news/2018/04/golf-is-the-no-1-u-s-sport-for-patents/>. Accessed: 27 Sept 2021.
6. United States Patent and Trademark Office. <https://www.uspto.gov/>. Accessed: 30 March 2022.
7. Farrally M et al (2003) Golf science research at the beginning of the twenty-first century. *J Sports Sci* 21:753-765. <https://doi.org/10.1080/0264041031000102123>
8. Penner AR (2003) The physics of golf. *Reports Progress Physics* 66:131-171. <https://doi.org/10.1088/0034-4885/66/2/202>
9. Betzler N, Monk S, Wallace E, Otto S, Shan G (2008) From the double pendulum model to full-body simulation: evolution of golf swing modeling. *Sports Tech* 1:175-188. <https://doi.org/10.1002/jst.60>
10. Wallace E, Kieran K, Strangwood M, Kenny I (2008) *Golf Science*. In: Reilly T (ed) *Science and Sports: Bridging the Gap*. Shaker Publishing. 94-107.
11. Jones K, Wallace E, Otto S (2018) Differences in the structure of variability in ground reaction force trajectories provide additional information about variability in the golf swing. *IMechE J Sports Eng Tech* 232:375-384. <https://doi.org/10.1177/1754337118772418>
12. Bourgain M, Sauret C, Rouillon O, Thoreux P, Rouch P (2017) Contribution of vertical and horizontal components of ground reaction forces on global motor moment during a golf swing: a preliminary study. *Comp Meth Biomech Biomed Eng* 20:S29-S30. <https://doi.org/10.1080/10255842.2017.1382845>
13. Peterson T, McNitt-Gray J (2018) Coordination of lower extremity multi-joint control strategies during the golf swing. *J Biomech* 77:26-33. <https://doi.org/10.1016/j.jbiomech.2018.06.004>
14. Hume PA, Keogh J (2017) Movement analysis of the golf swing. In: Müller B, Wolf S (eds) *Handbook of Human Motion*. Springer, Cham, 1-18. https://doi.org/10.1007/978-3-319-30808-1_137-1
15. Razavian RS, Greenberg S, McPhee J (2019) Biomechanics imaging and analysis. In: Narayan R (ed) *Encyclopedia of Biomedical Engineering*. Elsevier 2:488-500.
16. Chu Y, Sell TC, Lephart SM (2010) The relationship between biomechanical variables and driving performance during the golf swing. *J Sports Sci* 28:1251-1259. <https://doi.org/10.1080/02640414.2010.507249>
17. Lampsa, M (1975) Maximizing distance of the golf drive: an optimal control study. *J Dyn Sys Meas Control* 97:362-367. <https://doi.org/10.1115/1.3426951>
18. Choi A, Joo S-B, Oh E, Mun JH (2014) Kinematic evaluation of movement smoothness in golf: relationship between the normalized jerk cost of body joints and the clubhead. *Biomed Eng Online* 13:20. <http://www.biomedical-engineering-online.com/content/13/1/20>
19. Delphinus E, Sayers M (2012) Putting proficiency: contributions of the pelvis and trunk. *Sports Biomech* 11:212-222. <https://doi.org/10.1080/14763141.2011.638723>
20. Neal R, Lumsden R, Holland M, Mason B (2007) Body segment sequencing and timing in golf. *Int J Sports Sci Coach* 2:25-36. <https://doi.org/10.1260/174795407789705497>
21. Tinmark F, Hellström J, Halvorsen K, Thorstensson A (2010). Elite golfers' kinematic sequence in full-swing and partial-swing shots. *Sports Biomech* 9:236-244. <https://doi.org/10.1080/14763141.2010.535842>
22. MacKenzie SJ, Sprigings EJ (2009) A three-dimensional forward dynamics model of the golf swing. *Sports Eng* 11:165-175. <https://doi.org/10.1007/s12283-009-0020-9>
23. Seaman A, McPhee J (2012) Comparison of optical and inertial tracking of full golf swings. *Procedia Eng* 34:461-466. <https://doi.org/10.1016/j.proeng.2012.04.079>

24. Lai D, Hetchl M, Wei XC, Ball K, McLaughlin P (2011) On the difference in swing arm kinematics between low handicap golfers and non-golfers using wireless inertial sensors. *Procedia Eng* 13:219-225. <https://doi.org/10.1016/j.proeng.2011.05.076>
25. Chun S et al (2014) A sensor-aided self coaching model for uncocking improvement in golf swing. *Multimed Tools Appl* 72:253-279. <https://doi.org/10.1007/s11042-013-1359-2>
26. Lückemann P, Haid D, Brömel, Schwanitz S, Malwald C (2018) Validation of an inertial sensor system for swing analysis in golf. *Proceedings* 2:246. <https://doi.org/10.3390/proceedings2060246>
27. Kim M, Park S (2020) Golf swing segmentation from a single IMU using machine learning. *Sensors* 20:4466. <https://doi.org/10.3390/s20164466>
28. Goff J, Allen T (2020) Use of video for teaching sports mechanics, *Proceedings* 49:112. <https://doi.org/10.3390/proceedings2020049112>
29. Kanko R, Laende E, Strutzenberger G, Brown M, Selbie S, DePaul V, Scott S, Deluzio K (2021) Assessment of spatiotemporal gait parameters using a deep learning algorithm-based markerless motion capture system. *J. Biomech.*, 122:110414. <https://doi.org/10.1016/j.jbiomech.2021.110414>
30. Park S, Chang JY, Jeong H, Lee J-H, Park J-Y (2017) Accurate and efficient 3D human pose estimation algorithm using single depth images for pose analysis in golf. *IEEE CVPR Workshop, Honolulu, USA*, 105-113. <https://doi.org/10.1109/CVPRW.2017.19>
31. Lv D, Huang Z, Sun L, Yu N, Wu J (2017) Smart motion reconstruction system for golf swing: a DBN model based transportable, non-intrusive and inexpensive golf swing capture and reconstruction system. *Multimed Tools Appl* 76:1313-1330. <https://doi.org/10.1007/s11042-015-3102-7>
32. Mehta D et al (2017) VNect: Real-time 3D human pose estimation with a single RGB camera. *ACM Trans Graphics* 36:44. <https://doi.org/10.1145/3072959.3073596>
33. McNally W, Vats K, Pinto T, Dulhanty C, McPhee J, Wong A (2019) GolfDB: A Video Database for Golf Swing Sequencing. *IEEE/CVF Computer Vision in Sports, Long Beach, USA*, 2553-2562. <https://doi.org/10.1109/CVPRW.2019.00311>
34. Ko K-R, Pan SB (2021) CNN and bi-LSTM based 3D golf swing analysis by frontal swing sequence images. *Multimedia Tools Apps* 80:8957-8972. <https://doi.org/10.1007/s11042-020-10096-0>
35. McNally W, Vats K, Wong A, McPhee J (2022) Rethinking keypoint representations: modeling keypoints and poses as objects for multi-person human pose estimation. *Arxiv* 2111.08557. <https://doi.org/10.48550/arXiv.2111.08557>
36. Wang J et al (2021) Deep 3d human pose estimation: a review. *Comp Vision Image Understand* 210:103225. <https://doi.org/10.1016/j.cviu.2021.103225>
37. Koike S, Iida H, Shiraki H, Ae M (2006) An instrumented grip handle for golf clubs to measure forces and moments exerted by each hand during swing motion. *The Engineering of Sport* 6, Springer NY. https://doi.org/10.1007/978-0-387-46050-5_25
38. Budney D (1979) Measuring grip pressure during the golf swing. *Research Quart* 50:272-277. <https://doi.org/10.1080/10671315.1979.10615610>
39. Komi E, Roberts J, Rothberg S (2008) Measurement and analysis of grip force during a golf shot. *IMechE J Sports Eng Tech* 222:23-35. <https://doi.org/10.1243/17543371JSET9>
40. Barton B (2016) Smart, connected IoT golf grip with PGA Tour professional Bryson DeChambeau and Microsoft partner Sensoria. <https://microsoft.github.io/techcasestudies/iot/2016/11/23/senpga.html>. Accessed 11 April 2022.
41. McHardy A, Pollard H (2005) Muscle activity during the golf swing. *Brit. J. Sports Med.*, 39:799-804. <https://doi.org/10.1136/bjsm.2005.020271>
42. Marta S, Silva L, Castro M, Pezarat-Correia P, Cabri J (2012) Electromyography variables during the golf swing: a literature review. *J Electromyography*, 22:803-813. <http://dx.doi.org/10.1016/j.jelekin.2012.04.002>
43. Verikas A, Vaiciukynas E, Gelzinis A, Parker J, Charlotte Olsson M (2016) Electromyographic patterns during golf swing: activation sequence profiling and prediction of shot effectiveness. *Sensors*. 16:592. <https://doi.org/10.3390/s16040592>
44. Lagos L, Vaschillo E, Vaschillo B, Lehrer P, Bates M, Pandina R (2011) Virtual reality-assisted heart rate variability biofeedback as a strategy to improve golf performance: a case study. *Biofeedback* 39:15-20. <https://doi.org/10.5298/1081-5937-39.1.11>

45. Ji L, Wang H, Zheng TQ, Hua CC, Zhang NN (2019) Correlation analysis of EEG alpha rhythm is related to golf putting performance. *Biomed Signal Proc Control* 49:124-136. <https://doi.org/10.1016/j.bspc.2018.11.009>
46. The R&A, USGA (2019) The equipment rules. <https://www.usga.org/equipment-standards/equipment-rules-for-2019.html>. Accessed 31 March 2022.
47. Lückemann, Forrester S, Mears A, Shepherd J, Roberts J (2020) Assessment of measurement uncertainty in optical marker tracking of high-speed motion. *Proceedings* 49:72. <https://doi.org/10.3390/proceedings2020049072>
48. Betzler N, Kratzenstein S, Schweizer F, Witte K, Shan G (2006) 3D motion analysis of golf swings: development and validation of a golf-specific test set-up. 9th Symposium on 3D Analysis of Human Movement, Valenciennes, France. <http://www.univ-valenciennes.fr/congres/3D2006/>
49. Ellis K, Roberts J, Sanghera J (2010) Development of a method for monitoring clubhead path and orientation through impact. *Procedia Eng* 2:2955-2960. <https://doi.org/10.1016/j.proeng.2010.04.094>
50. Betzler N, Monk S, Wallace E, Otto S (2012) Variability in clubhead presentation characteristics and ball impact location for golfers' drives. *J Sports Sci* 30:439-448. <https://doi.org/10.1080/02640414.2011.653981>
51. Corke T, Betzler N, Wallace E, Otto S (2019) A novel system for tracking iron golf clubheads. *J Sports Eng Tech* 233:59-66. <https://doi.org/10.1177/1754337118792798>
52. Wood P, Henrikson E, Broadie C (2018) The influence of face angle and club path on the resultant launch angle of a golf ball. *Proceedings* 2:249. <https://doi.org/10.3390/proceedings2060249>
53. Haeufle D, Worobets J, Wright I, Haeufle J, Stefanyshyn D (2012) Golfers do not respond to changes in shaft mass properties in a mechanically predictable way. *Sports Eng* 14:215-220. <https://doi.org/10.1007/s12283-012-0104-9>
54. Pickering WM, Vickers GT (1999) On the double pendulum model of the golf swing. *Sports Eng* 2:161-172. <https://doi.org/10.1046/j.1460-2687.1999.00028.x>
55. Worobets J, Stefanyshyn D (2012) The influence of golf club shaft stiffness on clubhead kinematics at ball impact. *Sports Biomech* 11:239-248. <https://doi.org/10.1080/14763141.2012.674154>
56. Mase T, Timms M, West C (2006) Player fitting of golf equipment using a calibration club. *The Engineering of Sport* 6, Springer NY, 341-346.
57. McNally W, McPhee J (2020) Investigating the influence of shaft balance point on clubhead speed: a simulation study. *Proceedings* 49:156. <https://doi.org/10.3390/proceedings2020049156>
58. Mackenzie S, Henrikson E (2018) Influence of toe-hang versus face-balanced putter design on golfer applied kinetics. *Proceedings* 2:244. <https://doi.org/10.3390/proceedings2060244>
59. Shimizu T et al (2009) An analysis of the putter face control mechanism in golf putting. *Sports Eng* 12:21-30. <https://doi.org/10.1007/s12283-009-0025-4>
60. Betzler N, Monk S, Wallace E, Otto S (2012) Effects of golf shaft stiffness on strain, clubhead presentation and wrist kinematics. *Sports Biomech* 11:223-238. <https://doi.org/10.1080/14763141.2012.681796>
61. MacKenzie S, Boucher D (2018) The influence of golf shaft stiffness on grip and clubhead kinematics. *J Sports Sci* 35:105-111. <https://doi.org/10.1080/02640414.2016.1157262>
62. MacKenzie SJ, Spriggs EJ (2009) Understanding the role of shaft stiffness in the golf swing. *Sports Eng* 12:13-19. <https://doi.org/10.1007/s12283-009-0028-1>
63. McNally W, Henrikson E, McPhee J (2019) A continuous analytical shaft model for fast dynamic simulation of the golf swing. *Sports Eng* 22:20. <https://doi.org/10.1007/s12283-019-0314-5>
64. Milne R, Davis J (1992) The role of the golf shaft in the golf swing. *J Biomech* 25:975-983. [https://doi.org/10.1016/0021-9290\(92\)90033-W](https://doi.org/10.1016/0021-9290(92)90033-W)
65. Newman S, Clay S, Strickland P (1997) The dynamic flexing of a golf club shaft during a typical swing. *IEEE Conf Mechatronics Mach Vision Practice* 265-270. <https://doi.org/10.1109/MMVIP.1997.625343>
66. Betzler N, Slater C, Strangwood M, Monk S, Otto S, Wallace E (2011) The static and dynamic stiffness behaviour of composite golf shafts and their constituent materials. *Sports Eng* 14:27-37. <https://doi.org/10.1007/s12283-011-0068-1>

67. Jones K, Betzler N, Wallace E, Otto S (2019) Differences in shaft strain patterns during golf drives due to stiffness and swing effects. *Sports Eng* 22:14. <https://doi.org/10.1007/s12283-019-0308-3>
68. King K, Yoon S, Perkins N, Najafi K (2008) Wireless MEMS inertial sensor system for golf swing dynamics. *Sensors Act A* 141:619-630. <https://doi.org/10.1016/j.sna.2007.08.028>
69. Jensen U, Schmidt M, Hennig M, Dassler F, Jaitner T, Eskofier B (2015) An IMU-based mobile system for golf putt analysis. *Sports Eng* 18:123-133. <https://doi.org/10.1007/s12283-015-0171-9>
70. Couceiro M, Araújo A, Pereira S (2015) InPutter: an engineered putter for on-the-fly golf putting analysis. *Sports Tech* 8:12-29. <https://doi.org/doi:10.1080/19346182.2015.1064129>
71. Jiao L, Wu H, Bie R, Umek A, Kos A (2018) Multi-sensor golf swing classification using deep CNN. *Procedia Comp Sci* 129:59-65. <https://doi.org/10.1016/j.procs.2018.03.046>
72. Lombardo L, Iannucci L, Gullino A (2018) An inertial-based system for golf assessment. *Int Instrum Measure Tech Conf* 1-6. <https://doi.org/10.1109/I2MTC.2018.8409822>
73. Marquardt C (2007) The SAM PuttLab: concept and PGA tour data. *Int J Sports Sci Coach* 2:101-120. <https://doi.org/10.1260/174795407789705479>
74. Karlens J, Smith G, Nilsson J (2008) The stroke has only a minor influence on direction consistency in golf putting among elite players. *J Sports Sci* 26:243-250. <https://doi.org/10.1080/02640410701530902>
75. Sherwin I, Kenny I (2017) Putting movement and performance outcome using standard, belly and long putters. *Int J Sports Sci Coach* 12:532-539. <https://doi.org/10.1177/1747954117717880>
76. MacKenzie S, Evans D (2010) Validity and reliability of a new method for measuring putting stroke kinematics using the TOMI system. *J Sports Sci* 28:891-899. <https://doi.org/10.1080/02640411003792711>
77. Ferguson S, McNally W, McPhee J (2022) Predicting the Flight of a Golf Ball: Comparing a Physics-Based Aerodynamic Model to a Neural Network. *The Engineering of Sport* 14, USA.
78. Leach R, Forrester S, Mears A, Roberts J (2017) How valid and accurate are measurements of golf impact parameters obtained using commercially available radar and stereoscopic optical launch monitors? *Measurement* 112:125-136. <https://doi.org/10.1016/j.measurement.2017.08.009>
79. MacKenzie S, Ryan B, Rice A (2015) The influence of clubhead mass on clubhead and golf ball kinematics. *Int J Golf Sci* 4:136-146. <http://dx.doi.org/10.1123/ijgs.2015-0011>
80. Stefanyshyn D, Wannop J (2015) Biomechanics research and sport equipment development. *Sports Eng* 18:191-202. <https://doi.org/10.1007/s12283-015-0183-5>
81. Vena A, Budney D, Forest T, Carey J (2011) Three-dimensional kinematic analysis of the golf swing using instantaneous screw axis theory, Part 2: golf swing kinematic sequence. *Sports Eng* 13:125-133. <https://doi.org/10.1007/s12283-010-0059-7>
82. Uchida T, Delp S (2020) *Biomechanics of Movement*. MIT Press, USA.
83. Willams D (1967) The dynamics of the golf swing. *Quart J Mech Appl Math*, XX:247-264. <https://doi.org/10.1093/qjmam/20.2.247>
84. Cochran AJ, Stobbs J (1968) *The search for the perfect swing*. Morrison & Gibb Ltd, London
85. Vaughan C (1981) A three-dimensional analysis of the forces and torques applied by a golfer during the downswing. In: Morecki A, Fidelus K, Kedzior K, Witt A, eds. *Biomechanics VII-B*. University Park Press: Baltimore, USA. 325-331.
86. Neal R, Wilson B (1985) 3D Kinematics and kinetics of the golf swing. *Int J Sport Biomech*. 1:221-232. <https://doi.org/10.1123/ijsb.1.3.221>
87. Nesbit S et al (1996) A discussion of iron golf club head inertia tensors and their effects on the golfer. *J Appl Biomech* 12:449-469. <https://doi.org/10.1123/jab.12.4.449>
88. Sandhu S, Millard M, McPhee J, Brekke D (2010) 3D dynamic modelling and simulation of a golf drive. *Procedia Eng* 2:3243-3248. <https://doi.org/10.1016/j.proeng.2010.04.139>
89. Furukawa K, Tsujiuchi N, Ito A, Matsumoto K, Ueda M, Okazaki K (2018) The influence of the grip acceleration on club head rotation during a golf swing. *Proceedings* 2:241. <https://doi.org/10.3390/proceedings2060241>

90. Tanaka K, Sekizawa K (2018) Construction of a finite element model of golf clubs and influence of shaft stiffness on its dynamic behavior. *Proceedings* 2:247. <https://doi.org/10.3390/proceedings2060247>
91. Nesbit S (2007) Development of a full-body biomechanical model of the golf swing. *Int J Model Sim* 27:392-404. <https://doi.org/10.1080/02286203.2007.11442442>
92. Demircan E, Besier T, Khatib O (2012) Muscle force transmission to operational space accelerations during elite golf swings. *IEEE Int. Conf. Robotics Automation*, Saint Paul, Minnesota, USA. <https://doi.org/10.1109/ICRA.2012.6225336>
93. Smith A, Roberts J, Wallace E, Kong P, Forrester S (2016) Comparison of two- and three-dimensional methods for analysis of trunk kinematic variables in the golf swing. *J Appl Biomech* 32:23-31. <https://doi.org/10.1123/jab.2015-0032>
94. Bourgain M, Hybois S, Thoreux P, Rouillon O, Rouch P, Sauret C (2018) Effect of shoulder model complexity in upper-body kinematics analysis of the golf swing. *J. Biomech* 75:154-158. <https://doi.org/10.1016/j.jbiomech.2018.04.025>
95. Choi H, Park S (2020) Three dimensional upper limb joint kinetics of a golf swing with measured internal grip force. *Sensors* 20:3672. <https://doi.org/10.3390/s20133672>
96. Takagi T, Murata M, Yokozawa T, Shiraki H (2021) Dynamics of pelvis rotation about its longitudinal axis during the golf swing, *Sports Biomech* 20:583-602. <https://doi.org/10.1080/14763141.2019.1585472>
97. Shourijeh M, Mehrabi N, McPhee J (2017) Forward static optimization in dynamic simulation of human musculoskeletal systems: a proof-of-concept study. *ASME J Comput Nonlin Dyn* 12:051005. <https://doi.org/10.1115/1.4036195>
98. Jorgensen T (1994) *The physics of golf*. AIP Press, New York.
99. Chen C, Inoue Y, Shibara K (2007) Numerical study on the wrist action during the golf downswing. *Sports Eng* 10:23-31. <https://doi.org/10.1007/BF02844199>
100. Suzuki S, Haake S, Heller B (2006) Multiple modulation torque planning for a new golfswing robot with a skilful wrist turn. *Sports Eng* 9:201-228. <https://doi.org/10.1007/BF02866058>
101. Suzuki S, Hoshino Y, Kobayashi Y (2009) Skill analysis of the wrist release in the golf swings utilizing shaft elasticity. *J Sys Design Dyn* 3:47-58. <https://doi.org/10.1299/jsdd.3.47>
102. Lee C, Park S (2018) Estimation of unmeasured golf swing of arm based on the swing dynamics. *Int J Precision Eng Manu* 19:745-751. <https://doi.org/10.1007/s12541-018-0089-9>
103. McGuan A (1996) Exploring human adaptation using optimized, dynamic human models. 20th Annual Meeting of American Society of Biomechanics, Atlanta, USA.
104. Kenny IC, McCloy AJ, Wallace ES, Otto SR (2008) Segmental sequencing of kinetic energy in a computer-simulated golf swing. *Sports Eng* 11:37-45. <https://doi.org/10.1007/s12283-008-0005-0>
105. Choppin S, Allen T (2012) Special issue on predictive modelling in sport. *IMechE J Sports Eng Tech* 226:75-76. <https://doi.org/10.1177/1754337112443933>
106. Rao A (2009) A survey of numerical methods for optimal control. *Advances Astro Sci* 135:497-528.
107. Campbell K, Reid R (1985) The application of optimal control theory to simplified models of complex human motions: the golf swing. In: Winter D, Norman R, Wells R, Hayes K, Patla A, eds. *Biomechanics IX-B. Human Kinetics*: Baltimore, MD; 527-538.
108. Kaneko Y, Sato F (2000) The adaptation of golf swing to inertia property of golf club. In: Subic A, Haake S, eds. *The Engineering of Sport*. Blackwell Science, London 469-476.
109. Ming A, Mita T, Dhlamini S, Kajitani M (2001) Motion control skill in human hyper dynamic manipulation: an investigation on the golf swing by simulation. *Proceedings IEEE Comp Intel Rob Auto* 47-52. <https://doi.org/10.1109/CIRA.2001.1013171>
110. Sharp R (2009) On the mechanics of the golf swing. *Proc R Society A* 465:551-570. <https://doi.org/10.1098/rspa.2008.0304>
111. Sprigings E, Neal R (2000) An insight into the importance of wrist torque in driving the golfball: a simulation study. *J Appl Biomech* 16:356-366. <https://doi.org/10.1123/jab.16.4.356>
112. MacKenzie SJ, Sprigings EJ (2010) Understanding the mechanisms of shaft deflection in the golf swing. *Sports Eng* 12:69-75. <https://doi.org/10.1007/s12283-010-0034-3>

113. Balzerson D, Banerjee J, McPhee J (2016) A three-dimensional forward dynamic model of the golf swing optimized for ball carry distance. *Sports Eng* 19:237–250. <https://doi.org/10.1007/s12283-016-0197-7>
114. Yamaguchi G (2001) *Dynamic Modeling of Musculoskeletal Motion*. Springer USA. <https://doi.org/10.1007/978-0-387-28750-8>
115. Brown C, McNally W, McPhee J (2020) Optimal control of joint torques using direct collocation to maximize ball carry distance in a golf swing. *Multibody Sys Dyn* 50:323–333. <https://doi.org/10.1007/s11044-020-09734-0>
116. McNally W, McPhee J (2018) Dynamic optimization of the golf swing using a six degree-of-freedom biomechanical model. *Proceedings* 2:243. <https://doi.org/10.3390/proceedings2060243>
117. Ferguson S, McNally W, McPhee J (2022) The effect of club length, face bulge radius, and center of gravity depth on optimal golf drives – a simulation study. *Engineering of Sport* 14, USA.
118. Ezati M, Ghannadi B, McPhee J (2019) A review of simulation methods for human movement dynamics with emphasis on gait. *Multibody Sys Dyn* 47:265–292. <https://doi.org/10.1007/s11044-019-09685-1>
119. USGA and R&A (2021) A review of driving distance - 2021.
120. Gilardi G, Sharf I (2002) Literature survey of contact dynamics modelling. *Mech Mach Theory* 37:1213–1239. [https://doi.org/10.1016/S0094-114X\(02\)00045-9](https://doi.org/10.1016/S0094-114X(02)00045-9)
121. Corral et al (2021) Nonlinear phenomena of contact in multibody systems dynamics: a review. *Nonlin Dyn* 104:1269–1295. <https://doi.org/10.1007/s11071-021-06344-z>
122. Daish CB (1972) *The physics of ball games*. The English Universities Press, UK.
123. Brach R (1991) *Mechanical impact dynamics: rigid body collisions*. John Wiley and Sons, USA.
124. Winfield D, Tan T (1994) Optimization of clubhead loft and swing elevation angles for maximum distance of a golf drive. *Comp Struct* 53:19–25. [https://doi.org/10.1016/0045-7949\(94\)90125-2](https://doi.org/10.1016/0045-7949(94)90125-2)
125. Penner AR (2001) The physics of golf: the optimum loft of a driver. *Amer J Physics* 69:563–568. <https://doi.org/10.1119/1.1344164>
126. Penner AR (2001) The physics of golf: the convex face of a driver. *Amer J Physics* 69:1073–1081. <https://doi.org/10.1119/1.1380380>
127. Petersen W, McPhee J (2008) Comparison of impulse-momentum and finite element models for impact between golf ball and clubhead. *World Scientific Congress of Golf V*, Arizona, USA, 477–485.
128. Dewhurst P (2015) *The Science of the Perfect Swing*. Oxford Univ Press.
129. Lindsay N (2003) Topspin in putters — a study of vertical gear-effect and its dependence on shaft coupling. *Sports Eng* 6:81–93. <https://doi.org/10.1007/BF02903530>
130. Brouillette M (2010) Putter features that influence the rolling motion of a golf ball. *Procedia Eng* 2:3223–3229. <https://doi.org/10.1016/j.proeng.2010.04.136>
131. Lambeth J, Brekke D, Brunski J (2020) Exploration of center of gravity, moment of inertia, and launch direction for putters with ball speed normalizing face properties. *Proceedings* 49:2. <https://doi.org/10.3390/proceedings2020049002>
132. Cross R, Dewhurst P (2018) Launch speed, angle and spin in golf. *Eur J Physics* 39:065003. <https://doi.org/10.1088/1361-6404/aadda8>
133. Cross R (2002) Grip-slip behavior of a bouncing ball. *Amer J Physics* 70:1093–1102. <https://doi.org/10.1119/1.1507792>
134. Cross R, Nathan A (2009) Performance versus moment of inertia of sporting implements. *Sports Tech* 2:7–15. <https://doi.org/10.1002/jst.88>
135. McNally W, McPhee J, Henrikson E (2018) The golf shaft’s influence on clubhead-ball impact dynamics. *Proceedings* 2:245. <https://doi.org/10.3390/proceedings2060245>
136. Danaei B, McNally W, Henrikson E, McPhee J (2020) Adjusting a momentum-based golf clubhead-ball impact model to improve accuracy. *Proceedings* 49:47. <https://doi.org/10.3390/proceedings2020049047>
137. Caldwell A, McPhee J (2022) Comparison of Three-dimensional Dynamic Models for Golf Clubhead-ball Impacts. *The Engineering of Sport* 14, USA.
138. Tanaka K, Sato F, Oodaira H, Teranishi Y, Sato F, Ujihashi S (2006) Construction of the finite-element models of golf balls and simulations of their collisions. *IMechE J Materials Design App* 220:13–22. <https://doi.org/10.1243/14644207JMDA80>

139. Chou PC, Liang D, Yang J, Gobush W (1994) Contact forces, coefficient of restitution, and spin rate of golf ball impact. World Scientific Congress of Golf II, St. Andrews, Scotland, 359-365.
140. Tavares G, Sullivan M, Nesbitt D (1999) Use of finite element analysis in design of multilayer golf balls. World Scientific Congress of Golf III, St. Andrews, Scotland, 473-480.
141. Iwatsubo T, Kawamura S, Kazuyoshi M, Yamaguchi T (2000) Numerical analysis of golf club head and ball at various impact points. *Sports Eng* 3:195-204. <https://doi.org/10.1046/j.1460-2687.2000.00055.x>
142. Tanaka K, Oodaira H, Teranishi Y, Sato F, Ujihashi S (2009) Finite-element analysis of the collision and bounce between a golf ball and simplified clubs. In: *The Engineering of Sport 7*. Springer, France 653-662.
143. Nakai K, Wu Z, Sogabe Y, Arimitsu Y (2004) A study of thickness optimization of golf club heads to maximize release velocity of balls. *Commun Num Meth Eng* 20:747-755. <https://doi.org/10.1002/cnm.698>
144. Petersen W, McPhee J (2009) Shape optimization of golf clubface using finite element impact models. *Sports Eng* 12:77-85. <https://doi.org/10.1007/s12283-009-0030-7>
145. Wu Z, Tamaogi T, Sogabe Y, Arimitsu Y (2017) Design optimization of golf clubhead and ball with numerical analysis. *Global J Research Eng* 17:23-29.
146. Mase T, Sharpe R, Volkoff-Shoemaker N, Moreira S (2012) Modeling the sound of a golf club. *IMEchE J Sports Eng Tech* 226:107-113. <https://doi.org/10.1177/1754337112442782>
147. Delaye et al (2016) Modelling the sound of a golf ball impacting a titanium plate. *Procedia Eng* 147:354;359. <https://doi.org/10.1016/j.proeng.2016.06.309>
148. Roberts J, Jones R, Mansfield N, Rothberg S (2005) Evaluation of impact sound on the 'feel' of a golf shot. *J Sound Vib* 287:651-666. <https://doi.org/10.1016/j.jsv.2004.11.026>
149. Hunt K, Crossley E (1975) Coefficient of restitution interpreted as damping in vibroimpact. *J Appl Mech* 42:440-445. <https://doi.org/10.1115/1.3423596>
150. Brown P, McPhee J (2018) A 3D ellipsoidal volumetric foot-ground contact model for forward dynamics. *Multibody Sys Dyn* 42:447-467. <https://doi.org/10.1007/s11044-017-9605-4>
151. Lieberman B, Johnson S (1994) An analytical model for ball-barrier impact, Part 1: Models for normal impact. World Scientific Congress of Golf II, St. Andrews, Scotland, 375-380.
152. Johnson S, Lieberman B (1994) An analytical model for ball-barrier impact, Part 2: A model for oblique impact. World Scientific Congress of Golf II, St. Andrews, Scotland, 381-387.
153. Cochran A (2002) Development and use of one-dimensional models of a golf ball. *J Sports Sci* 20:635-641. <https://doi.org/10.1080/026404102320183202>
154. Arakawa K et al (2009) Dynamic deformation behavior of a golf ball during normal impact. *Exp Mech* 49:471-477. <https://doi.org/10.1007/s11340-008-9156-y>
155. Arakawa K (2014) Effect of time derivative of contact area on dynamic friction. *Appl Physics Letters* 104:241603. <https://doi.org/10.1063/1.4884055>
156. Arakawa K (2017) An analytical model of dynamic sliding friction during impact. *Sci Reports*. 7:40102. <https://doi.org/10.1038/srep40102>
157. Gonthier Y, McPhee J, Lange C (2007) On the implementation of Coulomb friction in a volumetric-based model for contact dynamics. *ASME Int Design Eng Tech Conf*, Las Vegas, USA, 423-432. <https://doi.org/10.1115/DETC2007-35311>
158. Brown P, McPhee J (2016) A continuous velocity-based friction model for dynamics and control with physically meaningful parameters. *ASME J Comput Nonlin Dyn* 11:054502. <https://doi.org/10.1115/1.4033658>
159. Maw N, Barber J, Fawcett J (1976) The oblique impact of elastic spheres. *Wear* 38:101-114. [https://doi.org/10.1016/0043-1648\(76\)90201-5](https://doi.org/10.1016/0043-1648(76)90201-5)
160. USGA and R&A (2006) Interim report: study of spin generation.
161. Henriksen E, Wood P, Broadie C, Nuttall T (2020) The role of friction and tangential compliance on the resultant launch angle of a golf ball. *Proceedings* 49:27. <https://doi.org/10.3390/proceedings2020049027>
162. Ma J et al (2021). A data-driven normal contact force model based on artificial neural network for complex contacting surfaces. *Mech Sys Sig Proc* 156:107612. <https://doi.org/10.1016/j.ymssp.2021.107612>

-
163. Penner AR (2002) The run of a golf ball. *Can J Physics* 80:931-940. <https://doi.org/10.1139/p02-035>
 164. USGA and R&A (2021) Proposed bounce model for use in evaluating optimum overall distance.
 165. Haake SJ (1989) Apparatus and test methods for measuring the impact of golf balls on turf and their application in the field. PhD Thesis, Aston University, UK.
 166. Roh W-J, Lee C-W (2010) Golf ball landing, bounce and roll on turf. *Procedia Eng* 2:3237-3242. <https://doi.org/10.1016/j.proeng.2010.04.138>
 167. Hubbard M, Alaways L (1998) Mechanical interaction of the golf ball with putting greens. *World Scientific Congress of Golf III*, St. Andrews, Scotland 429-439.
 168. Holmes B (1986) Dialogue concerning the stimp meter. *The Physics Teacher* 24:401-404. <https://doi.org/10.1119/1.2342065>
 169. Daemi N, Henning S, Gibert J, Yuya P, Ahmadi G (2016) On generalized rolling of golf balls considering an offset center of mass and rolling resistance: a study of putting. *Sports Eng* 19:35-46. <https://doi.org/10.1007/s12283-015-0186-2>
 170. Holmes B (1991) Putting: how a golf ball and hole interact. *Amer J Physics* 59:129-135. <https://doi.org/10.1119/1.16592>
 171. Kuchnicki S (2021) Interaction of a golf ball with the flagstick and hole. *Sports Eng* 24:8 <https://doi.org/10.1007/s12283-021-00347-0>
 172. Mase T (2019) <https://www.golfdigest.com/story/the-science-behind-why-the-flagstick-should-be-pulled-999-percent-of-the-time>. Accessed: 15 Sept 2021